

Liquidus Phase Relations on the Join Diopside-Forsterite-Anorthite From 1 atm to 20 kbar: Their Bearing on the Generation and Crystallization of Basaltic Magma*

D.C. Presnall**, Selena A. Dixon, James R. Dixon, T.H. O'Donnell***, N.L. Brenner****, R.L. Schrock*****, and D.W. Dycus*****

Department of Geosciences, University of Texas at Dallas, P.O. Box 688, Richardson, Texas 75080, USA

Abstract. In the system $\text{CaO-MgO-Al}_2\text{O}_3\text{-SiO}_2$, the tetrahedron $\text{CaMgSi}_2\text{O}_6$ (*di*)- Mg_2SiO_4 (*fo*)- SiO_2 - $\text{CaAl}_2\text{SiO}_6$ (*CaTs*) forms a simplified basalt tetrahedron, and within this tetrahedron, the plane *di-fo*- $\text{CaAl}_2\text{Si}_2\text{O}_8$ (*an*) separates simplified tholeiitic from alkalic basalts. Liquidus phase relations on this join have been studied at 1 atm and at 7, 10, 15, and 20 kbar. The temperature maximum on the 1 atm isobaric quaternary univariant line along which forsterite, diopside, anorthite, and liquid are in equilibrium lies to the SiO_2 -rich side of the join *di-fo-an*. The isobaric quaternary invariant point at which forsterite, diopside, anorthite, spinel, and liquid are in equilibrium passes, with increasing pressure, from the silica-poor to the silica-rich side of the join *di-fo-an*, which causes the piercing points on this join to change from forsterite + diopside + anorthite + liquid and forsterite + spinel + anorthite + liquid below 5 kbar to forsterite + diopside + spinel + liquid and diopside + spinel + anorthite + liquid above 5 kbar. As pressure increases, the forsterite and anorthite fields contract and the diopside and corundum fields expand. The anorthite primary phase field disappears entirely from the join *di-fo-an* between 15 and 20 kbar. Below about 4 kbar, the join *di-fo-an* represents, in simplified form, a thermal divide between alkalic and tholeiitic basalts. From about 4 to at least 12 kbar, alkalic

basalts can produce tholeiitic basalts by fractional crystallization, and at pressures above about 12 kbar, it is possible for alkalic basalt to be produced from oceanite by crystallization of both olivine and orthopyroxene. If alkalic basalts are primary melts from a lherzolite mantle, they must be produced at high pressures, probably greater than about 12 kbar.

Introduction

About 85% of the chemical constituents of basalt and about 90% of the chemical constituents of the upper mantle are contained in the system $\text{CaO-MgO-Al}_2\text{O}_3\text{-SiO}_2$; and with the exception of nepheline, representatives of all the major anhydrous minerals found in basalts and in the upper mantle are present (forsterite, enstatite, diopside, anorthite, spinel, pyrope, grossular, melilite). Because this system contains only 4 components, it is possible to represent geometrically the compositional relations among the various crystalline and liquid phases. Because of these features, the system $\text{CaO-MgO-Al}_2\text{O}_3\text{-SiO}_2$ is an excellent model system for studying basalt crystallization trends and the generation of basalts from the mantle.

Yoder and Tilley (1962) presented a classification for basalts based on the normative tetrahedron quartz-olivine-diopside-nepheline, and within this tetrahedron, the plane olivine-diopside-plagioclase has been considered to be a low-pressure thermal divide between tholeiitic and alkalic basalts (Yoder and Tilley, 1962; O'Hara, 1965, 1968). The existence of this thermal divide in nature is based on data from several simplified systems, one of the most important of which is *di-fo-an* (Fig. 1). In the system $\text{CaO-MgO-Al}_2\text{O}_3\text{-SiO}_2$, this join lies within the simplified basalt tetrahedron $\text{SiO}_2\text{-fo-di-CaTs}$. Osborn and Tait (1952) studied liquidus phase relations on the join *di-fo-an*

* Department of Geosciences, University of Texas at Dallas Contribution No. 327. Hawaii Institute of Geophysics Contribution No. 814.

** Present address: Hawaii Institute of Geophysics, University of Hawaii, Honolulu, HI 96822, USA

*** Present address: U.S. Geological Survey, 307 Federal Building, Ft. Myers, FL 33901, USA

**** Present address: Information Systems, Indiana University, Bloomington, IN 47401, USA

***** Present address: Geochemical Testing Inc., 149 Fuller St., Somerset, PA 15501, USA

***** Present address: University of Texas Health Science Center at Dallas, TX 75235, USA

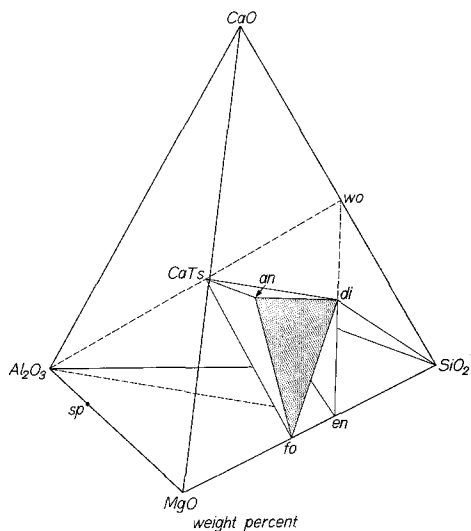


Fig. 1. The tetrahedron $\text{CaO-MgO-Al}_2\text{O}_3\text{-SiO}_2$ with the simplified basalt tetrahedron fo-di-CaTs-SiO_2 . The plane studied here is shaded and the plane of aluminous pyroxene compositions is dashed. fo =forsterite (Mg_2SiO_4), di =diopside ($\text{CaMgSi}_2\text{O}_6$), an =anorthite ($\text{CaAl}_2\text{Si}_2\text{O}_8$), en =enstatite (MgSiO_3), wo =wollastonite (CaSiO_3), CaTs =Ca Tschermak's molecule ($\text{CaAl}_2\text{SiO}_6$), sp =spinel (MgAl_2O_4)

at 1 atm, and in this paper, a small refinement of their study is presented together with liquidus phase relations at 7, 10, 15 and 20 kbar. The results show the effect of pressure on this simplified thermal divide and, by extrapolation, on crystallization trends in basaltic magmas.

Experimental Method

Many of the starting mixtures are the same as those used in the original study at 1 atm by Osborn and Tait (1952), and were generously made available by Osborn. A few of the mixtures were prepared in our laboratory using starting materials described by Presnall et al. (1972). For the new compositions, ten grams of each oxide mixture were fired in a platinum crucible for 4 h at about 1650° C and quenched to a glass. The crushed glass powders served as starting materials for the equilibrium experiments.

Runs were carried out in a solid media piston-cylinder apparatus similar to that described by Boyd and England (1960), with a pressure-cell arrangement identical to that described by Presnall et al. (1973). To insure that charges were free of water, all parts of the pressure cell except the talc sleeve were dried for one hour at 1050° C and then stored in a desiccator prior to an experiment. The platinum capsules were loaded, dried with the other pressure-cell parts, and then closed. All experiments were of the decompression or "piston-out" type and were carried out by initially overpressurizing the sample by about 4 kbar, raising the temperature to the desired value, and then bleeding to the required pressure. No pressure correction was applied. Based on comparisons with gas-apparatus measurements, it is believed that this procedure closely approximates the actual pressure on the sample, at least for the high temperature conditions reported here (Presnall, 1976, p. 585). Except as indicated in the tables, Pt/Pt10Rh thermocouples

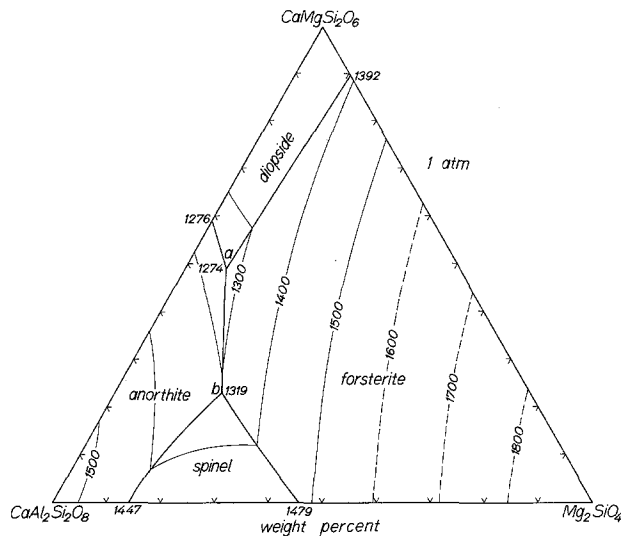


Fig. 2. Liquidus phase relations in the join $\text{CaMgSi}_2\text{O}_6\text{-Mg}_2\text{SiO}_4\text{-CaAl}_2\text{Si}_2\text{O}_8$ at 1 atm, redrawn after Osborn and Tait (1952), Hytönen and Schairer (1961), Kushiro and Schairer (1963), and Kushiro (1972a). Heavy lines are boundary lines and light lines are liquidus isotherms with temperatures in °C

were used and no pressure correction was applied to the thermocouple readings. All temperatures including those of previous workers have been corrected to conform to the International Practical Temperature Scale of 1968 (Anonymous, 1969). Phases were identified by microscopic examination of polished thin sections of the quenched charges, and compositions of phases were determined with an ARL-EMX-SM electron microprobe. Correction of the raw electron microprobe data for absorption, fluorescence, and atomic number effects was accomplished using the EMPADR VII computer program of Rucklidge and Gasparrini (1969). Electron microprobe standards were a diopside glass, one enstatite glass containing 10 wt% Al_2O_3 , and another containing 20 wt% Al_2O_3 , all obtained from F.R. Boyd.

Phase Relations at One Atm

Figure 2 shows the join $\text{CaMgSi}_2\text{O}_6\text{-Mg}_2\text{SiO}_4\text{-CaAl}_2\text{Si}_2\text{O}_8$ at 1 atm as determined by Osborn and Tait (1952), with slight revisions by Hytönen and Schairer (1961), Kushiro and Schairer (1963), and Kushiro (1972a). The adjustments to the phase boundaries and liquidus isotherms of Osborn and Tait are minor and do not change the positions of the two ternary piercing points located by them.

In Figure 3, the quaternary univariant line along which liquid is in equilibrium with forsterite, anorthite, and diopside (line $a-p$) passes through the plane di-fo-an at the piercing point a . If forsterite, diopside, and anorthite showed no solid solution, a temperature maximum on this line would lie exactly in the plane di-fo-an , and the phase relations (exclud-

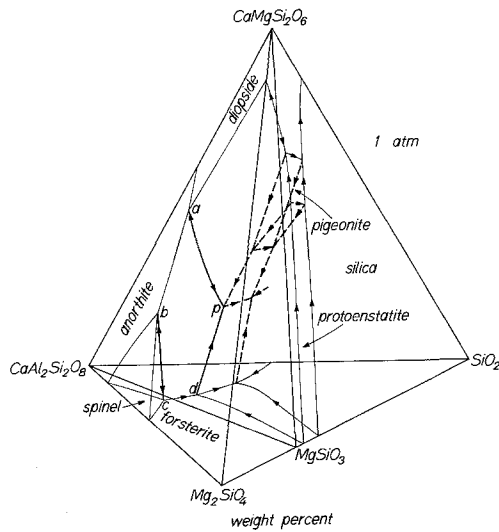


Fig. 3. Liquidus phase relations in the tetrahedron $\text{CaMgSi}_2\text{O}_6$ - Mg_2SiO_4 - $\text{CaAl}_2\text{Si}_2\text{O}_8$ - SiO_2 at 1 atm. Compiled from Bowen (1914), Andersen (1915), Osborn and Tait (1952), Hytönen and Schairer (1960, 1961), Kushiro and Schairer (1963), Kushiro (1972a), Yang (1973), and Presnall et al. (in press). Light lines are liquidus boundary lines on the faces of the tetrahedron, and heavy lines (dashed where inferred) are quaternary liquidus univariant lines. Arrows indicate directions of decreasing temperature. The back face, $\text{CaMgSi}_2\text{O}_6$ - $\text{CaAl}_2\text{Si}_2\text{O}_8$ - SiO_2 , although determined by Clark, Schairer, and de Neufville (1962) is omitted for clarity

Table 1. Runs at one atmosphere, all on the composition 46% $\text{CaMgSi}_2\text{O}_6$, 7% Mg_2SiO_4 , 47% $\text{CaAl}_2\text{Si}_2\text{O}_8$ (wt%)

Run No.	Temp. (°C)	Time (h)	Phases Present ^a
56	1276	26	gl+an
55	1272	15	gl+an+fo+di
57	1266	24	gl+an+fo+di
58	1263	48	gl+an+fo+di

^a an=anorthite, fo=forsterite, di=diopside, gl=glass

Table 2. Microprobe analyses of glasses at one atmosphere (wt%)

Run No. ^a	55	57
Spots Analyzed	3	9
SiO ₂	48.51 ± 0.04 ^b	46.80 ± 0.43 ^b
Al ₂ O ₃	15.87 ± 0.20	15.46 ± 0.22
MgO	13.34 ± 0.12	12.92 ± 0.08
CaO	22.40 ± 0.19	23.17 ± 0.58
Total	100.12	98.35
fo	6.12	4.22
di	52.72	57.59
an	43.25	42.89
SiO ₂ ^c	-2.09	-4.70

^a Run numbers are keyed to Table 1
^b Standard deviation
^c (-) means deficiency

Table 3. Microprobe analyses of diopsides (wt%).

Run No. ^a	55	98-5
Pressure	1 atm	10 kbar
SiO ₂	54.79 ± 0.04 ^b	50.07 ± 0.18 ^b
Al ₂ O ₃	2.97 ± 0.04	10.57 ± 0.26
MgO	19.43 ± 0.15	17.39 ± 0.06
CaO	24.16 ± 0.02	22.56 ± 0.23
Total	101.35	100.59
fo	5.57	9.29
di	85.84	64.29
an	8.00	28.68
SiO ₂ ^c	+0.58	-2.25

No. of Atoms for 6 Oxygens

Si	1.938	} 2.000	1.779	} 2.000
Al	0.062		0.221	
Al	0.062	} 2.002	0.221	} 1.999
Mg	1.024		0.857	
Ca	0.916	0.921		

^a Run numbers are keyed to Tables 1 and 5
^b Maximum deviation (2 crystals)
^c (+) means excess, (-) means deficiency

ing the spinel field) would be ternary. However, because the compositions of diopside and forsterite lie off the join, the temperature maximum on the liquidus univariant line also lies off the join. Hytönen and Schairer (1961) and Chinner and Schairer (1962) placed the maximum to the silica-rich side of the plane *di-fo-an* but O'Hara and Schairer (1963) placed it to the silica-poor side.

In order to resolve this discrepancy, we have performed some additional experiments on the composition 46% $\text{CaMgSi}_2\text{O}_6$, 7% Mg_2SiO_4 , 47% $\text{CaAl}_2\text{Si}_2\text{O}_8$ (Table 1). Because this mixture lies exactly on a line between the anorthite corner and point *a*, crystallization of anorthite drives the liquid path straight to point *a* where diopside and forsterite both appear simultaneously. At this point, the liquid path still lies on the join *di-fo-an*, and if further cooling causes complete crystallization of the mixture, the temperature maximum on the quaternary univariant line must lie exactly on the join *di-fo-an*. As shown in Table 1, however, liquid persists below the temperature of point *a* down to at least 1263° C, indicating that crystallization of diopside, forsterite, and anorthite drives the liquid path off the join. Our temperature for point *a* (1274° C) agrees within experimental uncertainty with that of Osborn and Tait (1272° C). We have analyzed the composition of the glass at 1272° C and 1266° C, and as shown in Table 2, both compositions lie to the silica-poor side of the join

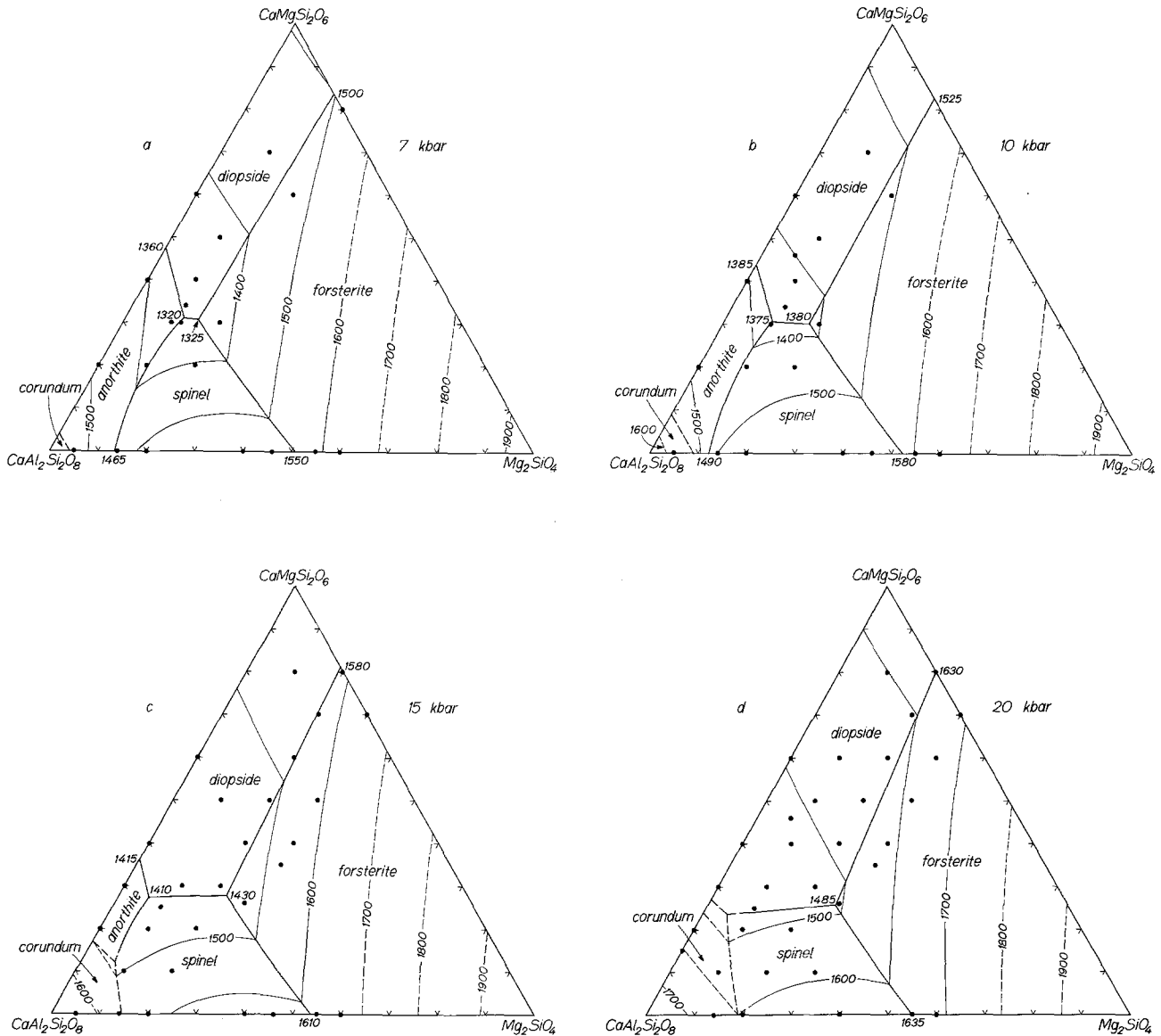


Fig. 4a-d. Liquidus phase relations on the join $\text{CaMgSi}_2\text{O}_6$ - Mg_2SiO_4 - $\text{CaAl}_2\text{Si}_2\text{O}_8$ at 7, 10, 15, and 20 kbar (wt%). Filled circles are compositions studied. Heavy lines (dashed where equilibrium not demonstrated) are liquidus boundary lines and light lines (dashed where inferred or equilibrium not demonstrated) are liquidus isotherms. Temperatures are in $^{\circ}\text{C}$

di-fo-an, with the SiO_2 deficiency increasing as temperature falls. This confirms that the temperature maximum lies on the silica-rich side, in agreement with the conclusion of Hytönen and Schairer (1961) and Chinner and Schairer (1962). We have also analyzed the diopside composition in run 55 at 1272°C (Table 3) and found that it lies very close to and slightly to the silica-rich side of the join *di-fo-an*. The forsterite in run 55 contains a small amount of CaO (0.77 wt%) and lies on the SiO_2 -poor side of the join *di-fo-an*. Crystallization of forsterite thus tends to counteract the effect of crystallization of diopside, but as shown by the glass analyses in Table 2, the

net effect is to drive the liquid toward the SiO_2 -poor side of the join *di-fo-an*.

Phase Relations at High Pressures

Liquidus surfaces for the join $\text{CaMgSi}_2\text{O}_6$ - Mg_2SiO_4 - $\text{CaAl}_2\text{Si}_2\text{O}_8$ at 7, 10, 15, and 20 kbar are shown in Figure 4a-d, and data used in constructing these diagrams are listed in Tables 4, 5, 6, and 7. Melting temperatures for Mg_2SiO_4 at the various pressures are taken from Davis and England (1964), and those for

Table 4. Runs at 7 kbar

Run No.	Composition (wt%)			Temp. (°C)	Time (h)	Phases Present ^a
	CaMgSi ₂ O ₆	Mg ₂ SiO ₄	CaAl ₂ Si ₂ O ₈			
72-1	0	5	95	1520	4	<i>gl</i>
104-13				1492	6	<i>gl+an</i>
71-7	0	14	86	1468	4	<i>gl</i>
72-3				1443	4	<i>gl+sp+an</i>
60-4	0	20	80	1531	3	<i>gl</i>
59-4				1515	3	<i>gl+sp</i>
45-8	0	40	60	1572	2	<i>gl</i>
42-3				1554	2	<i>gl+sp</i>
52-6	0	46	54	1572	2	<i>gl</i>
47-11				1546	2	<i>gl+sp</i>
98-4	0	55	45	1614	4	<i>gl</i>
96-4				1588	4	<i>gl+fo+q(fo)</i>
97-1	0	60	40	1614	4	<i>gl+q(fo)</i>
96-1				1598	4	<i>gl+fo+q(fo)</i>
127-1	20	0	80	1480	6	<i>gl</i>
129-2				1460	6	<i>gl+an</i>
77-2	20	10	70	1365	6	<i>gl</i>
89-1				1339	4	<i>gl+an</i>
59-7	20	20	60	1443	3	<i>gl</i>
58-6				1417	3	<i>gl+sp</i>
71-1	30	10	60	1365	4	<i>gl</i>
72-11				1339	4	<i>gl+an+di+sp</i>
109-21	30	12	58	1375	5	<i>gl</i>
108-7				1350	4	<i>gl+sp</i>
97-7	30	20	50	1396	4	<i>gl</i>
96-5				1370	4	<i>gl+fo</i>
92-14				1344	4	<i>gl+fo</i>
94-3				1324	4	<i>gl+fo+di</i>
96-8				1324	4	<i>gl+fo+di+sp</i>
110-5	34	11	55	1340	4	<i>gl</i>
110-2				1335	4	<i>gl+an+di</i>
57-7	40	0	60	1443	4	<i>gl</i>
72-5				1417	4	<i>gl+an</i>
98-8	40	10	50	1365	4	<i>gl</i>
97-5				1339	4	<i>gl+di</i>
97-4	50	10	40	1365	4	<i>gl</i>
98-6				1339	4	<i>gl+di</i>
78-5	60	0	40	1391	6	<i>gl</i>
58-2				1365	2	<i>gl+di</i>
124-1	60	20	20	1480 ^b	6	<i>gl</i>
124-4				1455 ^b	5	<i>gl+fo+q(fo)</i>
53-8	70	10	20	1453	2	<i>gl</i>
51-11				1427	2	<i>gl+di+q(di)</i>
98-3	80	20	0	1546	4	<i>gl</i>
97-6				1520	4	<i>gl+fo+q(fo)</i>

^a Abbreviations as in Table 1 except *sp*=spinel, *q*=quench crystals with types of quench crystals in parentheses^b W3Re/W25Re thermocouple

Table 5. Runs at 10 kbar

Run No.	Composition (wt%)			Temp. (°C)	Time (h)	Phases Present ^a
	CaMgSi ₂ O ₆	Mg ₂ SiO ₄	CaAl ₂ Si ₂ O ₈			
70-3	0	5	95	1572	4	<i>gl</i>
72-2				1546	4	<i>gl</i> + <i>cor</i>
71-4	0	14	86	1520	4	<i>gl</i>
72-4				1494	4	<i>gl</i> + <i>sp</i>
59-3	0	20	80	1577	3	<i>gl</i>
58-5				1551	3	<i>gl</i> + <i>sp</i>
54-2	0	40	60	1624	2	<i>gl</i>
52-5				1598	2	<i>gl</i> + <i>sp</i>
55-1	0	46	54	1629	2	<i>gl</i>
54-3				1603	2	<i>gl</i> + <i>sp</i>
92-8	0	55	45	1624	4	<i>gl</i>
89-3				1598	4	<i>gl</i> + <i>fo</i> + <i>q(fo)</i>
97-2	0	60	40	1639	4	<i>gl</i>
98-7				1614	4	<i>gl</i> + <i>fo</i> + <i>q(fo)</i>
61-2	20	0	80	1520	4	<i>gl</i>
61-1				1494	4	<i>gl</i> + <i>an</i>
74-7	20	10	70	1417	4	<i>gl</i>
77-3				1391	6	<i>gl</i> + <i>an</i> + <i>sp</i>
94-5	20	20	60	1468	4	<i>gl</i>
47-14				1468	2	<i>gl</i> + <i>sp</i>
71-2	30	10	60	1391	4	<i>gl</i>
67-9				1365	4	<i>gl</i> + <i>an</i> + <i>sp</i>
89-6	30	20	50	1417	4	<i>gl</i>
96-7				1396	4	<i>gl</i> + <i>fo</i>
92-9				1370	4	<i>gl</i> + <i>fo</i>
98-5				1344	4	<i>gl</i> + <i>fo</i> + <i>di</i> + <i>sp</i> + <i>q(di)</i>
96-9				1324	4	<i>gl</i> + <i>fo</i> + <i>di</i> + <i>sp</i>
110-19	34	11	55	1375	4	<i>gl</i>
110-6				1360	4	<i>gl</i> + <i>di</i>
72-7	40	0	60	1443	4	<i>gl</i>
71-3				1417	4	<i>gl</i> + <i>an</i>
45-11	40	10	50	1417	2	<i>gl</i>
44-12				1391	2	<i>gl</i> + <i>di</i>
94-2	46	7	47	1391	4	<i>gl</i>
94-1				1365	4	<i>gl</i> + <i>di</i> + <i>q(di)</i>
52-12	50	10	40	1417	2	<i>gl</i>
94-7				1391	4	<i>gl</i> + <i>di</i> + <i>q(di)</i>
79-6	60	0	40	1417	6	<i>gl</i>
92-1				1391	4	<i>gl</i> + <i>di</i>
96-2	60	20	20	1525	4	<i>gl</i>
92-10				1500	4	<i>gl</i> + <i>fo</i> + <i>q(fo)</i>
52-16	70	10	20	1494	2	<i>gl</i> + <i>q(di)</i>
92-11				1468	4	<i>gl</i> + <i>di</i> + <i>q(di)</i>

^a Abbreviations as in Table 4 except *cor*=corundum

Table 6. Runs at 15 kbar

Run No.	Composition (wt%)			Temp. (°C)	Time (h)	Phases Present ^a
	CaMgSi ₂ O ₆	Mg ₂ SiO ₄	CaAl ₂ Si ₂ O ₈			
101-3	0	5	95	1660	4	<i>gl</i>
104-8				1634	4	<i>gl + cor</i>
101-2	0	14	86	1546	4	<i>gl</i>
100-1				1520	4	<i>gl + cor + sp</i>
102-8	0	20	80	1598	4	<i>gl</i>
99-5				1572	4	<i>gl + sp</i>
99-6	0	40	60	1650	4	<i>gl</i>
104-4				1624	4	<i>gl + sp + q(di)</i>
104-9	0	46	54	1650	4	<i>gl</i>
99-10				1624	4	<i>gl + sp + q(di)</i>
108-8	0	55	45	1623	4	<i>gl</i>
109-20				1600	4	<i>gl + fo + q(fo)</i>
100-6	0	60	40	1676	4	<i>gl</i>
106-8				1650	4	<i>gl + fo + q(fo)</i>
104-7	10	10	80	1520	4	<i>gl</i>
104-3				1494	4	<i>gl + sp</i>
104-10	10	10	70	1572	4	<i>gl</i>
103-2				1546	4	<i>gl + sp</i>
113-23	20	0	80	1490	6	<i>gl</i>
113-25				1465	6	<i>gl + an</i>
104-5	20	10	70	1468	4	<i>gl</i>
101-5				1443	4	<i>gl + sp</i>
103-1	20	20	60	1494	4	<i>gl</i>
102-4				1468	4	<i>gl + sp</i>
110-10	25	10	65	1450	4	<i>gl</i>
109-11				1425	4	<i>gl + sp + di + q(di)</i>
109-7	26	27	47	1450	4	<i>gl</i>
110-11				1435	4	<i>gl + fo + di + sp + q(di)</i>
111-15	30	0	70	1455	6	<i>gl</i>
111-7				1430	6	<i>gl + an</i>
106-6	30	12	58	1464	4	<i>gl</i>
105-8				1441	4	<i>gl + di + sp + q(di)</i>
113-12	30	20	50	1430	6	<i>gl</i>
113-10				1405	6	<i>gl + di + sp + q(di)</i>
105-4	35	30	35	1549	4	<i>gl</i>
105-9				1523	4	<i>gl + fo + q(fo)</i>
109-22				1460	4	<i>gl + fo + q(fo)</i>
106-4				1440	4	<i>gl + fo + di + sp + q(fo)</i>
113-22	40	0	60	1415	6	<i>gl</i>
103-4				1391	4	<i>gl + di + an</i>
99-9	40	20	40	1468	4	<i>gl</i>
85-4				1443	4	<i>gl + di + sp</i>
100-9	40	30	30	1598	4	<i>gl</i>
102-3				1572	4	<i>gl + fo + q(fo)</i>
85-8				1494	4	<i>gl + fo + q(fo)</i>
131-1	50	10	40	1480	4	<i>gl</i>
113-11				1455	6	<i>gl + di + q(di)</i>
113-14				1430	6	<i>gl + di + q(di)</i>
113-6	50	20	30	1495	6	<i>gl</i>
113-8				1470	6	<i>gl + di + fo + q(di)</i>

Table 6 (continued)

Run No.	Composition (wt%)			Temp. (°C)	Time (h)	Phases Present
	CaMgSi ₂ O ₆	Mg ₂ SiO ₄	CaAl ₂ Si ₂ O ₈			
100-4	50	30	20	1598	4	<i>gl</i>
103-7				1572	4	<i>gl+fo+q(fo)</i>
101-1	60	0	40	1443	4	<i>gl</i>
100-7				1417	4	<i>gl+di</i>
99-1	60	20	20	1520	4	<i>gl</i>
85-2				1494	4	<i>gl+fo+di+q(di)</i>
99-2	70	20	10	1572	4	<i>gl</i>
79-4				1546	5	<i>gl+fo+di</i>
101-9	70	30	0	1650	4	<i>gl+q(fo)</i>
104-1				1650	4	<i>gl+fo+q(fo)</i>
111-12	80	10	10	1550	4	<i>gl</i>
111-14				1525	4	<i>gl+di+q(di)</i>
85-3	80	20	0	1598	4	<i>gl+q(di)</i>
85-7				1572	4	<i>gl+fo+q(di, fo)</i>

^a Abbreviations as in Table 5

CaMgSi₂O₆ are taken from Boyd and England (1963). The diopside melting temperatures are essentially identical to those of Williams and Kennedy (1969) when the latter are uncorrected for the pressure effect on the thermocouple.

Liquidus temperatures for CaAl₂Si₂O₈ were estimated from Figure 1b of Lindsley (1968) after raising the liquidus curve about 50° C at 1 atm and 30° C at 20 kbar to correct a drafting error and make it consistent with his Figure 2 (Lindsley, personal communication). When this correction is made, the singular point at which anorthite begins to melt incongruently to corundum+liquid appears to occur at approximately 6 kbar. Hariya and Kennedy (1968) placed the singular point at 9 kbar, but they show a point in their Figure 3 at 7.3 kbar, 1570° C, in which corundum+liquid formed from anorthite. Some confusion exists, however, because this run is not indicated in their Table 3 as having formed corundum. The singular point is tentatively assumed to lie at about 6 kbar because this position fits better with data on the join *di-fo-an* reported here, but it should be noted that equilibrium has not been achieved in the corundum field even for runs lasting up to 50 h, as discussed below in the section on reversal experiments.

Three other relevant high pressure studies are those of Kushiro (1969a) and Kushiro and Yoder (1966, 1974). Kushiro (1969a) studied the join CaMgSi₂O₆-Mg₂SiO₄ at 20 kbar and placed the liquidus boundary between the diopside and forsterite primary phase fields at 23% Mg₂SiO₄, 77% CaMgSi₂O₆, and 1635° C. Our boundary at 20 kbar (Fig. 4d) is placed

at the same temperature but is moved slightly toward CaMgSi₂O₆ to 21% Mg₂SiO₄ to make it more compatible with our data. The new location is still within the uncertainty of Kushiro's data.

Kushiro and Yoder (1966) studied the composition CaMg₂Al₂Si₃O₁₂ (1:1 mole ratio of anorthite and forsterite) and found spinel on the liquidus over the entire pressure range from 1 atm to 30 kbar. We have not studied this composition, but their liquidus data are in agreement with Figure 4a-d.

The liquidus surface of the join MgSiO₃-CaSiO₃-Al₂O₃ (see Fig. 1) was studied by Kushiro and Yoder (1974) at 20 kbar. This plane intersects the plane studied here along the line CaMgSi₂O₆-CaMg₂Al₂Si₃O₁₂. In Figure 4d, a line (not shown) from CaMg₂Al₂Si₃O₁₂ (66.4% CaAl₂Si₂O₈, 33.6% Mg₂SiO₄) to CaMgSi₂O₆ would show the boundary between the spinel and diopside fields at 26% CaMgSi₂O₆, whereas in Figure 38 of Kushiro and Yoder (1974) this boundary is shown at about 16% CaMgSi₂O₆. This difference cannot be reconciled as experimental error but could possibly be explained as a difference in interpretation of the run products. For runs in the primary phase field of spinel, the equilibrium spinel crystals frequently form nucleation sites for diopside quench crystals that completely surround each spinel crystal (Table 7). Kushiro and Yoder may have extended the diopside field because they did not see the spinel and interpreted the diopside as equilibrium crystals.

The join *di-fo-an* is not ternary at any pressure, and to understand the phase relations completely it

Table 7. Runs at 20 kbar

Run No.	Composition (wt%)			Temp. (°C)	Time (h)	Phases Present ^a
	CaMgSi ₂ O ₆	Mg ₂ SiO ₄	CaAl ₂ Si ₂ O ₈			
111-1	0	14	86	1690	2	<i>gl</i>
110-1				1665	4	<i>gl+cor</i>
95-5	0	20	80	1598	4	<i>gl</i>
82-2				1572	4	<i>gl+sp</i>
95-13	0	40	60	1676	4	<i>gl</i>
93-3				1650	4	<i>gl+sp+q(di)</i>
87-6	0	55	45	1650	4	<i>gl</i>
109-14				1620	4	<i>gl+sp+fo+q(fo)</i>
82-3	0	60	40	1676	4	<i>gl</i>
108-11				1650	4	<i>gl+fo+q(fo)</i>
107-6	10	10	80	1572	4	<i>gl</i>
90-9				1546	4	<i>gl+cor</i>
90-3	10	20	70	1572	4	<i>gl</i>
87-11				1546	4	<i>gl+sp+q(di)</i>
108-9	10	30	60	1600	4	<i>gl</i>
91-3				1598	4	<i>gl+sp+q(di)</i>
118-9	15	0	85	1475 ^b	2+48 ^c	<i>gl</i>
123-2				1450 ^b	2+50 ^c	<i>gl</i>
118-7				1450 ^b	2+46 ^c	<i>gl+cor+di</i>
121-8	20	0	80	1500 ^b	3+48 ^c	<i>gl</i>
121-10				1475 ^b	3+49 ^c	<i>gl</i>
123-3				1450 ^b	2+50 ^c	<i>gl+cor</i>
109-18	20	10	70	1500	6	<i>gl</i>
113-20				1500	6	<i>gl+sp</i>
108-15	20	20	60	1540	4	<i>gl</i>
90-6				1546	4	<i>gl+sp+q(di)</i>
110-3	25	10	65	1475	6	<i>gl+q(di)</i>
110-12				1450	6	<i>gl+di+q(di)</i>
109-8	26	27	47	1530	4	<i>gl</i>
110-9				1505	4	<i>gl+di+fo+sp+q(di)</i>
111-6	30	0	70	1485	6	<i>gl</i>
111-3				1460	6	<i>gl+di+q(di)</i>
83-7	30	10	60	1494	4	<i>gl</i>
83-4				1468	4	<i>gl+di</i>
82-5	30	20	50	1494	4	<i>gl</i>
108-4				1470	4	<i>gl+di+sp+q(di)</i>
108-5	35	30	35	1570	4	<i>gl</i>
107-5				1546	4	<i>gl+fo+q(fo)</i>
81-3	40	0	60	1468	4	<i>gl</i>
113-17				1440	6	<i>gl+di+q(di)</i>
95-8	40	10	50	1494	4	<i>gl</i>
107-4				1468	4	<i>gl+di+q(di)</i>
82-1	40	20	40	1520	4	<i>gl</i>
108-6				1500	4	<i>gl+di+q(di)</i>
83-6	40	30	30	1598	4	<i>gl</i>
81-7				1572	4	<i>gl+fo+q(fo)</i>
107-3	46	7	47	1520	4	<i>gl</i>
95-15				1494	4	<i>gl+di+q(di)</i>
93-6	50	10	40	1546	4	<i>gl</i>
93-4				1520	4	<i>gl+di+q(di)</i>

Table 7 (continued)

Run No.	Composition (wt%)			Temp. (°C)	Time (h)	Phases Present
	CaMgSi ₂ O ₆	Mg ₂ SiO ₄	CaAl ₂ Si ₂ O ₈			
108-3	50	20	30	1570	4	<i>gl</i>
91-5				1546	4	<i>gl + di + q(di)</i>
91-6	50	30	20	1624	4	<i>gl</i>
91-2				1598	4	<i>gl + fo + q(fo)</i>
91-9	60	0	40	1494	4	<i>gl</i>
93-11				1468	4	<i>gl + di + q(di)</i>
95-14	60	10	30	1546	4	<i>gl + q(di)</i>
107-2				1520	4	<i>gl + di + q(di)</i>
95-2	60	20	20	1572	4	<i>gl</i>
93-2				1546	4	<i>gl + fo + di + q(di)</i>
108-4	60	30	10	1645	4	<i>gl</i>
91-7				1624	4	<i>gl + fo + q(fo)</i>
107-1	70	20	10	1598	4	<i>gl + q(di)</i>
95-9				1572	4	<i>gl + di + fo + q(di)</i>
93-8	70	30	0	1676	4	<i>gl + q(fo)</i>
87-5				1650	4	<i>gl + fo + q(fo)</i>
95-7	80	10	10	1598	4	<i>gl</i>
108-2				1570	4	<i>gl + di</i>
91-10	80	20	0	1624	4	<i>gl + q(di)</i>
93-5				1598	4	<i>gl + fo + di</i>

^a Abbreviations as in Table 5

^b W3Re/W25Re thermocouple

^c The first number indicates hours held at 1600° C and the second number indicates hours held at the temperature indicated for the run

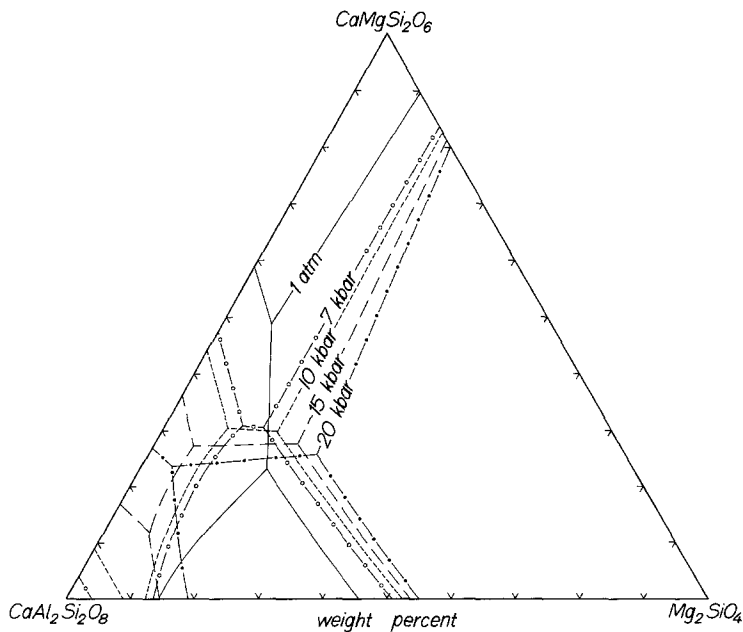


Fig. 5. Composite diagram showing changes in liquidus boundary lines with pressure

Table 8. Compositions of piercing points at various pressures (wt%)

P (kbar)	CaMgSi ₂ O ₆	Mg ₂ SiO ₄	CaAl ₂ Si ₂ O ₈
	<i>fo + di + sp + liq</i>		
7	30.7 ^a	15.3	54.0
10	30.0	18.0	52.0
15	27.8	22.3	49.9
20	25.7	26.4	47.9
	<i>di + sp + an + liq</i>		
7	31.0	12.0	57.0
10	30.6	10.0	59.4
15	27.4	6.2	66.4

^a These values only describe the positions of the points on Figure 4a-d. The number of digits is not related to uncertainties in the positions of the points

is necessary to use the tetrahedron CaO-MgO-Al₂O₃-SiO₂. However, some of the important changes with pressure can be seen in Figures 4 and 5. As pressure increases, the forsterite and anorthite fields contract, and the diopside and corundum fields expand. When the spinel field is in contact with the forsterite and anorthite fields, it expands as pressure increases, but when it is in contact with the diopside and corundum fields, it contracts with increasing pressure. Between 15 and 20 kbar, the anorthite primary phase field disappears entirely from this join.

At some pressure between 1 atm and 7 kbar (probably about 5 kbar), the quaternary isobaric invariant point involving the phases forsterite, diopside, anorthite, spinel, and liquid lies exactly on the join *di-fo-an*. As pressure increases, it moves from the silica-poor to the silica-rich side of this join, which causes the piercing points to change from forsterite + anorthite + diopside + liquid and forsterite + spinel + anorthite + liquid at 1 atm (Fig. 2) to forsterite + diopside + spinel + liquid and spinel + diopside + anorthite + liquid at 7 kbar (Fig. 4a). The positions of these latter two piercing points at 7 kbar and above are listed in Table 8.

Reversal Experiments

In order to prove that all the runs reported here were held long enough to reach equilibrium, it would be necessary to carry out a pair of reversal experiments for each liquidus bracket. This would have been an enormous task, so we have adopted the slightly less rigorous approach of reversing a few selected liquidus brackets. Other factors being equal, different crystalline phases tend to dissolve and crystallize at rates characteristic of the particular crystal-

line phase. Thus, reversal of a liquidus temperature in each of the primary phase fields was attempted. A reversal was accomplished by first bracketing the liquidus temperature with runs of, for example, 2 h. A second set of two runs was then made in which the sample was held in one case for 2 h above and in the other case for 2 h below the liquidus. Without taking the sample out of the apparatus, the temperature of each run was then changed to the other side of the liquidus and held for an additional 2 h. This technique constitutes a reversal that is independent of both the nature of the starting material and any changes that may occur while bringing the sample up to temperature and pressure. As shown in Table 9, successful reversals were achieved for the spinel, anorthite, diopside, and forsterite primary phase fields. Based on these results, all compositions in the primary phase fields of spinel and diopside were held for at least 2 h, and all compositions in the primary phase fields of anorthite and forsterite were held for at least 4 h. These are minimum times for attainment of equilibrium. Shorter runs frequently gave erroneous results.

Reversals were not done at 15 and 20 kbar. It has been assumed that run times established at low pressures, where viscosities of liquids are higher (Kushiro et al., 1976) and liquidus temperatures are lower, would be adequate also at higher pressures. Comparison of Tables 4, 5, 6, and 7 shows that quench crystals are more common at higher pressures, and confirms the assumption of more rapid reaction rates under these conditions.

The corundum liquidus presented severe problems and it was found impossible to obtain consistent results even with runs lasting up to 50 h. At 20 kbar, it was found that the compositions 15% CaMgSi₂O₆, 85% CaAl₂Si₂O₈ and 20% CaMgSiO₆, 80% CaAl₂Si₂O₈ would melt completely in two hours at 1600° C. Reversals in the down-temperature direction were then attempted by holding these mixtures for 2 to 3 h at 1600° C and then at various lower temperatures for 46 to 50 h (see Table 7). Corundum was produced but the liquidus temperatures for the two mixtures were not internally consistent. It was decided not to pursue the corundum field with longer runs because of the prolonged effort that would be required and the minimum relevance of the corundum field to problems of basalt genesis. In Tables 5, 6, and 7, shorter runs showing corundum are listed and the corundum fields in Figures 4a-d are based in an approximate way on these runs. However, because equilibrium may not have been attained, the liquidus isotherms and limiting boundary lines for the corundum field have been dashed. It was not possible to construct the diagrams so that they were consistent with all the corundum-bearing runs but the results

Table 9. Reversal experiments

Run No.	Composition (wt%)			Initial Conditions			Final Conditions			Phases Present ^a
	CaMgSi ₂ O ₆	Mg ₂ SiO ₄	CaAl ₂ Si ₂ O ₈	T (°C)	P (kbar)	Time (h)	T (°C)	P (kbar)	Time (h)	
45-1	0	40	60	1546	7	2	1572	7	2	<i>gl</i>
46-1	0	40	60	1572	7	2	1520	7	2	<i>gl+sp</i>
59-1	20	0	80	1484	10	3	1531	10	3	<i>gl</i>
71-8	20	0	80	1531	10	3	1484	10	4	<i>gl+an</i>
52-1	60	0	40	1401	10	2	1443	10	2	<i>gl</i>
52-2	60	0	40	1443	10	2	1401	10	2	<i>gl+di</i>
92-4	0	20	80	1494	10	4	1520	10	4	<i>gl+q(fo)</i>
92-5	0	20	80	1520	10	4	1494	10	4	<i>gl+fo+q(fo)</i>

^a Abbreviations as in Table 4

are reported in case they may be of some value in future studies.

Minimum Pressure Required for the Formation of Primary Alkalic¹ Basalt Magma

After olivine, the most commonly occurring mineral in many suites of mantle nodules is orthopyroxene, and orthopyroxene is generally considered to be an important constituent of the mantle source material from which basaltic magmas are derived (for example, see Green and Ringwood, 1967; O'Hara, 1968; Yoder, 1976). If alkalic basalt is a primary magma type, as argued by Green and Ringwood (1967), Kushiro (1968), and Yoder (1976), and if it is the result of a small amount of partial fusion (Green and Ringwood, 1967; Gast, 1968), then alkalic basalt must be in equilibrium with orthopyroxene at its source region.

As mentioned above and as shown from numerous other studies (Boyd et al., 1964; Green and Ringwood, 1967; Kushiro, 1968; Chen and Presnall, 1975), the olivine primary phase field becomes smaller as pressure increases and the boundary between the olivine and enstatite fields moves toward the alkalic basalt volume. If alkalic basalts are to be generated as primary melts, the enstatite field must eventually penetrate the alkalic basalt volume, which means, for

¹ In the discussions that follow, the term alkalic basalt will refer to compositions that contain normative olivine and hypersthene (*fo* and *en* in the simplified tetrahedron). Although Na₂O and K₂O are absent from the simplified system, compositions within the tetrahedron *di-fo-an-CaTs* will nevertheless be referred to as alkalic in the sense that they lie on the silica-poor side of the "critical plane of silica undersaturation" of Yoder and Tilley (1962)

simplified basalts in the system CaO-MgO-Al₂O₃-SiO₂, it must penetrate the plane *di-fo-an*. It can be seen in Figure 4 that no enstatite field exists, and if the enstatite field penetrates this plane, it must do so at some pressure greater than 20 kbar.

We now inquire to what extent other components would modify this minimum pressure estimate of 20 kbar for the generation of primary alkalic basalt magma. Kushiro (1972b) found in the system Na₂O-CaO-MgO-Al₂O₃-SiO₂ that liquids in equilibrium with olivine, enstatite, diopside, and spinel (spinel lherzolite assemblage) are olivine normative at 10 kbar and nepheline normative at 20 kbar, a result similar to his earlier findings for the system Mg₂SiO₄-SiO₂-NaAlSiO₄ (Kushiro, 1968). Melting experiments on natural lherzolites (Mysen and Kushiro, 1977) indicate that at 20 kbar, a small amount of fusion (1.77% for the lherzolite 1611) produces nepheline normative liquids and a large amount (15.7% for the lherzolite 1611), produces hypersthene normative liquids. Other data (Kushiro, 1972b, 1973a and b) are compatible with this same interpretation at both 15 and 20 kbar, although in these other studies the amount of fusion was not carefully determined. Green and Ringwood (1967, Fig. 6) have reported that orthopyroxene crystallizes from an alkali olivine basalt at 13.5 kbar but not at 9 kbar. The data of Green and Ringwood (1967) are controversial (Mysen and Boettcher, 1975, pp. 577-578; Yoder, 1976, p. 148), but if their results are taken at face value and combined with the other data on fusion of lherzolites, the minimum pressure for the penetration of the enstatite field into the alkalic basalt volume, and thus for the generation of alkalic basalts as primary melts, would be 10 to 13.5 kbar. In subsequent discussions, the mid-point of this range, 12 kbar, will be taken as the *approximate* minimum

pressure, but it is evident from the above discussion that this estimate may be subject to revision.

Thus, the addition of other components causes the enstatite field to shift toward more alkalic compositions and reduces the pressure at which alkalic basalts can be generated as primary magmas. O'Hara (1965, 1968) hypothesized that the enstatite field penetrates the alkalic basalt volume at a pressure of 8 to 10 kbar, but in view of the above discussion, his estimate appears to be slightly low. The minimum pressure estimate of 12 kbar would be raised by the presence of H₂O and lowered by the presence of CO₂ (Kushiro, 1972c; Egglar, 1973, 1974; Mysen and Boettcher, 1975).

The Join CaMgSi₂O₆-Mg₂SiO₄-CaAl₂Si₂O₈ as a Thermal Divide at One Atm

Because the compositions of diopside, spinel, and forsterite all lie off the join *di-fo-an*, liquid crystallization paths for starting compositions close to this plane are complex, and the plane can be thought of only in an approximate sense as a simplified low-pressure thermal divide between tholeiitic and alkalic basalts. In order to define the exact shape of the thermal divide, it would be necessary to have detailed data on the compositions of the crystalline phases in equilibrium with various liquids in the vicinity of the plane *di-fo-an*. Such data are not available, but some general statements can nevertheless be made.

In Figure 2, the spinel field defines a window through which liquid paths originating on the alkalic side of the join *di-fo-an* can fractionate to the tholeiitic side by crystallization of spinel either alone or together with forsterite or anorthite. A different relationship exists when spinel is in equilibrium with both forsterite and anorthite. In Figure 3, a temperature maximum is shown on the line *b-c*, and comparison with the location of spinel in Figure 1 shows that a reaction relation exists along this line in which spinel dissolves while anorthite and forsterite crystallize. During equilibrium crystallization, tholeiitic liquids could move a short distance along this line toward the plane *di-fo-an*, but no liquid path originating from a tholeiitic starting composition could cross this plane along line *b-c* and move to alkalic compositions. This is because the tetrahedral volume defined by the apices *fo*, *an*, *sp*, and a liquid on the extension of *b-c* to the SiO₂-poor side of *di-fo-an* would not contain tholeiitic bulk compositions. During fractional crystallization of a liquid on the reaction line *b-c*, the liquid path would not move along *b-c* at all but would move out onto the anorthite-forsterite boundary surface (*a-b-c-d-p*) toward higher SiO₂ contents.

If it is assumed that anorthite and forsterite show no solid solution (forsterite actually contains a small amount of CaO), compositions outside the spinel field but within the triangular region *Mg₂SiO₄-CaAl₂Si₂O₈-b* (Fig. 2) would initially crystallize either forsterite or anorthite. The liquid paths would then move to the boundary of the spinel field where crystallization of either forsterite+spinel or anorthite+spinel would drive the liquid paths into the tholeiite volume (Fig. 3). Similar crystallization behavior would be shown by a limited range of adjacent compositions within the alkalic basalt volume (Fig. 1).

In an approximate way, that portion of Figure 2 exclusive of the triangular region *Mg₂SiO₄-CaAl₂Si₂O₈-b* can be thought of as a system with a simple ternary eutectic and therefore a thermal divide. However, because the forsterite contains a small amount of CaO, its composition lies slightly to the SiO₂-poor side of the plane *di-fo-an* and fractional crystallization of compositions in the primary phase field of forsterite in Figure 2 would produce liquid paths deviating slightly from the plane *di-fo-an* toward the SiO₂-rich side. Conversely, it can be seen in Table 3 that the diopside composition at point *a* (Figs. 2 and 3) lies to the SiO₂-rich side of the plane *di-fo-an* and fractional crystallization of at least some of the compositions in the diopside field of Figure 2 would drive liquid paths to the SiO₂-poor side. When anorthite, forsterite, and diopside all crystallize together, the thermal divide is located within the tholeiitic basalt volume at the temperature maximum on the line *a-p* (Fig. 3).

Thus, part of the join *di-fo-an* corresponds approximately to a thermal divide between alkalic and tholeiitic basalts, and part is a window through which alkalic compositions can fractionate to tholeiitic compositions by crystallization of spinel. The thermal divide portion is a complex curved surface that lies mainly within the tholeiitic basalt volume but partly (because forsterite shows solid solution toward monticellite) within the alkalic basalt volume.

Disappearance of the Thermal Divide at High Pressures

Yoder and Tilley (1962) pointed out that the thermal divide between tholeiitic and alkalic basalt at 1 atm is broken at high pressures (greater than 20 kbar) because of the appearance of garnet and jadeitic pyroxene. O'Hara (1965, 1968) hypothesized later that the thermal divide disappears at about 8 kbar, a pressure well below the appearance of garnet at liquidus temperatures. For the join *di-fo-an*, it is now possible to discuss in detail the changing phase relationships that cause the disappearance of the thermal divide.

The position of the temperature maximum on line $a-p$ (Fig. 3) is strongly dependent on the diopside composition, and as the diopside becomes increasingly aluminous and SiO_2 -poor at higher pressures (Table 3), the position of the temperature maximum (and the complex curved surface defining the thermal divide) moves from the SiO_2 -rich to the SiO_2 -poor side of the plane $di-fo-an$. Also, as pressure rises, the isobaric quarternary invariant point involving forsterite, diopside, anorthite, spinel, and liquid passes from the SiO_2 -poor to the SiO_2 -rich side of the join $di-fo-an$. This causes points a and b (Figs. 2 and 3) to approach each other, meet at about 5 kbar as the isobaric invariant point passes across the join, and then separate at higher pressures as two new piercing points (Figs. 4a-d and 5). At some pressure less than 5 kbar, the temperature maximum meets the invariant point and thereby disappears, taking with it the thermal divide. The pressure at which the temperature maximum disappears has not been determined but is probably in the vicinity of 3 kbar. Thus, in a narrow pressure range from about 3 to 5 kbar, the univariant line along which forsterite, diopside, and anorthite crystallize penetrates the join $di-fo-an$, with temperature decreasing continuously from the SiO_2 -poor to the SiO_2 -rich side of this join, and crystallization of these three phases from a simplified alkalic basalt would yield simplified tholeiitic residual liquids.

At pressures from about 5 kbar up to at least 20 kbar, the isobaric quaternary univariant line along which forsterite, diopside, spinel, and liquid are in equilibrium forms a piercing point as it passes through the plane $di-fo-an$ (Fig. 4a-d). Temperatures along this line decrease from the alkalic to the tholeiitic side. At 10 kbar, the composition of the diopside at the piercing point has been determined (Table 3) and from this information it is apparent that a reaction relation exists in which olivine dissolves as spinel and aluminous diopside crystallize. Because of lack of data on the diopside composition at other pressures, it is not possible to determine the pressure range over which the reaction relation persists; but regardless of this uncertainty, fractional crystallization of alkalic liquids on the univariant line forsterite + diopside + spinel + liquid will produce tholeiitic residual liquids by crystallization of either diopside and spinel at pressures where the reaction relation exists or forsterite, diopside, and spinel at pressures where it may not exist.

Another isobaric univariant line penetrates the join $di-fo-an$ from about 5 to 18 kbar, and produces the piercing point at which diopside, spinel, anorthite, and liquid are in equilibrium (Fig. 4a-c). Again, temperature decreases along this line toward the tholeiitic side of the join $di-fo-an$. Data are insufficient to deter-

mine if a reaction relation exists for this line, but it is probable that none exists at lower pressures near 5 kbar. At higher pressures (Fig. 4c), the piercing point moves toward the $di-an$ side of the diagram, which probably results in a reaction relation in which aluminous diopside and anorthite crystallize as spinel dissolves. Fractional crystallization of simplified alkalic basalts by crystallization of either aluminous diopside, anorthite, and spinel at lower pressures or aluminous diopside and anorthite at higher pressures would again produce tholeiitic residual liquids.

Thus, for simplified basalt compositions, the join $di-fo-an$ corresponds approximately to a thermal divide between alkalic and tholeiitic compositions up to about 3 kbar as long as spinel does not crystallize, but at all higher pressures up to at least 20 kbar, fractional crystallization can produce tholeiitic from alkalic liquids. Some data are available on the effect of Na_2O on this thermal divide. Kushiro (1968), in his study of the system Mg_2SiO_4 - SiO_2 - NaAlSiO_4 at high pressures, showed that the thermal divide between Mg_2SiO_4 and $\text{NaAlSi}_3\text{O}_8$ does not exist at 10 kbar, and it appears from interpolation of his data that the divide breaks at about 5 kbar. The work of Kushiro is in agreement with the earlier study of Yoder (1964) at 9 kbar only if it is assumed that Yoder's phase diagram showing what he believed to be metastable phase relations (see his Fig. 25) actually shows stable phase relations. Thus, there is some uncertainty in the phase diagram for Mg_2SiO_4 - $\text{NaAlSi}_3\text{O}_8$ at high pressures, but if Kushiro's data are accepted, it appears that the pressure at which the divide is broken is raised only slightly, perhaps to 4 kbar, by the presence of Na_2O . The effect of iron is not known precisely but is probably small (Kushiro, 1975). Thus, the available data indicate that for complex rock compositions, the thermal divide between tholeiitic and alkalic basalt is a feature that is important only for fractional crystallization taking place near the earth's surface.

Fractional Crystallization of Basaltic Magma at Low and Intermediate Pressures

It was noted above that for complex natural compositions, the orthopyroxene primary phase field penetrates the alkalic basalt volume at approximately 12 kbar. Thus, the mechanisms discussed above for producing tholeiitic from alkalic basalt would apply only from about 4 to 12 kbar, and the consequences of fractional crystallization of a natural alkalic basalt at pressures above 12 kbar are not clarified by the data presented here.

The possibility of deriving tholeiitic from alkalic

basalt at 4–12 kbar is directly opposite to the fractionation trend implied by the hypothetical phase diagram of O'Hara (1965, Fig. 10; 1968) at 8–10 kbar. His diagram shows orthopyroxene, clinopyroxene, and plagioclase crystallizing to drive liquid paths from the tholeiitic to the alkalic volume. In the system $\text{CaO-MgO-Al}_2\text{O}_3\text{-SiO}_2$, a univariant line exists at these pressures along which enstatite, diopside, and anorthite are in equilibrium (Presnall, et al., in press), but the fractionation trend along this line is toward silica rather than away from silica as hypothesized by O'Hara.

The fractionation trend at 9 kbar calculated by Green and Ringwood (1967, Table 15 and Figs. 8 and 9) for their alkali olivine basalt moves away from the tholeiite field, a trend that might seem to be in conflict with the phase relationships presented here. However, their calculation assumed the crystallization of olivine and clinopyroxene at a temperature only about 50° C below the liquidus. Near the solidus temperature for this same basalt, they observed olivine, clinopyroxene, spinel, and plagioclase coexisting with liquid (see their Table 6, run 788). This assemblage is closely analogous to the assemblages at the two high-pressure piercing points on the join *di-fo-an*, one being forsterite + diopside + spinel + liquid (Fig. 4a–d), and the other being diopside + spinel + anorthite + liquid (Fig. 4a–c). Because comparisons between their results and the system $\text{CaO-MgO-Al}_2\text{O}_3\text{-SiO}_2$ are not exact, it is not certain that the liquid path in the complex composition would move from an alkalic to a tholeiitic composition, but this trend is likely to be produced by the crystallization of olivine, diopside, plagioclase, and spinel if the diopside is aluminous, as would be the case at 9 kbar, and if the alkalic parent liquid is already near the olivine-plagioclase-diopside plane. Thus, their calculation of a fractionation trend away from the tholeiite field at high temperatures is not in conflict with the possibility of a fractionation trend back toward a tholeiitic composition at lower temperatures involving different crystallizing phases.

Common phenocrysts in alkalic lavas are olivine, augite, and plagioclase, with magnetite sometimes being present (Macdonald and Powers, 1946). Thus, there is a close correspondence between the phase relations reported here, the near-solidus experiment of Green and Ringwood (1967), and phenocryst phases observed in natural alkalic rocks. Furthermore, in Hawaii, the sequence alkalic basalt-hawaiite-mugearite-trachyte ranges from nepheline-normative through hypersthene-normative to quartz-normative compositions (Macdonald and Katsura, 1964). Based on the data reported here, the nepheline to hypersthene normative portion of this trend could be

produced in the approximate pressure range of 4 to 12 kbar as the alkalic basalt magmas move upward to the surface, the remainder of the fractionation sequence possibly being produced at shallow depths directly beneath the volcano. Macdonald and Powers (1946) reported that olivine, augite, and plagioclase phenocrysts from alkalic lavas at Haleakala volcano, Hawaii are frequently partially resorbed, which is consistent with a moderate pressure origin for the initial stages of the alkalic differentiation sequence.

However, it is not intended to imply that all alkalic basalt magmas must fractionate on their way to the surface. As pointed out by Yoder (1976, pp. 147–148), many alkalic basalts are apparently erupted very rapidly from great depths because of the abundance of mantle nodules in these lavas. Kushiro et al. (1976) have calculated from viscosity data that a basalt bringing a peridotite nodule to the surface would have to rise from a depth of 50 km in less than 60 h. For these basalts, only very limited fractional crystallization would be possible during ascent to the surface.

In many areas, notably Hawaii, alkalic basalts follow production of the main tholeiitic shield, and this has commonly been taken as evidence that a fractionation trend from alkalic to tholeiitic basalt does not occur. However, there are a few localities where a differentiation trend from alkalic to tholeiitic basalt may have occurred. On Mull, tholeiitic basalts follow the eruption of alkalic basalts, although the large time interval between these flows may obviate a co-magmatic relationship (Carmichael et al., 1974, p. 460). In Skye, tholeiitic basalt has been reported to be sandwiched between alkalic flows (Thompson et al., 1972), but it is not clear that the entire sequence was produced from the same vent. Another possible example of a fractionation trend from alkalic to tholeiitic basalt has been reported in the Canary Islands (Ibarrola, 1969).

At higher pressures from 13.5 to 18 kbar, Green and Ringwood (1967) and Green (1969) have suggested that alkalic basalt could be derived from olivine-rich tholeiite by crystallization of aluminous enstatite. Derivation of alkalic from tholeiitic basalt by separation of orthopyroxene was suggested for Hawaiian lavas by Powers (1935, p. 67), Macdonald (1949, p. 1583) and Tilley (1950, p. 45), but this idea was later abandoned by Powers (1955, pp. 85, 95) (see also discussions by Yoder, 1964; Tilley and Yoder, 1964). O'Hara (1968, pp. 93–94) and Kushiro (1969b) have pointed out that the expansion of the olivine primary phase field as pressure drops causes extreme difficulties for an orthopyroxene fractionation scheme. If a basaltic magma is in equilibrium with olivine at its source region, the composition of the magma will lie within the olivine primary phase field

Table 10. Summary of possible crystal fractionation trends

Approximate Pressure (kbar)	Fractionation Trend
0-4	Thermal divide between tholeiitic and alkalic basalt except when the crystallizing phases include spinel, in which case alkalic basalt fractionates to tholeiite
4-12	Alkalic basalt fractionates to olivine tholeiite
> 12	Oceanite fractionates to alkalic basalt by crystallization of olivine and orthopyroxene. Derivative magmas produced by fractionation of alkalic basalt not determined

at all lower pressures as the magma moves upward to the surface. Thus, if fractional crystallization occurs, the magma cannot avoid crystallizing olivine. Because the enstatite primary phase field penetrates the alkalic basalt volume at these pressures, it is possible to produce alkalic basalt from tholeiite rich in normative olivine (oceanite), but the fractionation process would involve the crystallization of olivine as well as enstatite.

Engel et al. (1965) suggested that alkalic basalts are differentiated from tholeiitic basalts primarily by fractional crystallization, but arguments based on field studies, phase equilibrium relationships, and trace element data are all in agreement that low-pressure fractional crystallization does not produce this trend (Powers, 1955; Kuno, 1957; Yoder and Tilley, 1962; O'Hara, 1965, 1968; Green and Ringwood, 1967; Gast, 1968). The present data simply add greater weight to the argument that low-pressure fractional crystallization from tholeiitic to alkalic basalt is not possible. If such a fractionation trend occurs, it appears that it must take place at a pressure greater than about 12 kbar, and the tholeiitic parent must be rich in normative olivine and poor in normative plagioclase (oceanite), a composition very different from the mid-ocean ridge tholeiites rich in normative plagioclase assumed by Engel et al. (1965) to be parental.

Table 10 summarizes the fractionation trends for natural basalts at various pressures. This table does not indicate fractionation trends that *necessarily* occur, but rather trends that are *possible* given sufficient residence time of basaltic liquids at the appropriate pressures.

Effects of H₂O and CO₂

Very little mention has been made of the effect of volatiles on the liquidus phase relations at high pres-

ures. The most important volatile constituents in regions of magma generation are generally considered to be CO₂ and H₂O. Dramatic shifts in phase boundaries occur for systems studied at high pressures under water-saturated conditions (Kushiro, 1969a, 1972c), but at a pressure of 20 kbar, for example, water saturation would require silicate melts to contain roughly 15 wt% water (Kushiro, 1972c). Such a large amount is geologically unrealistic. Hart and Nalwalk (1970) found H₂O⁺ in fresh tholeiites from the ocean floor to be less than about 0.3 wt%. Moore (1970) found H₂O⁺ values less than about 0.4 wt% for mid-ocean ridge tholeiites and also maximum values of about 1.0 and 0.6 wt% for fresh underwater eruptions of alkalic basalt and Hawaiian tholeiite, respectively (see also Killingley and Muenow, 1975). If these percentages are representative of the amount of water in basaltic magmas at depth, the effect of water on at least the early and middle stages of fractional crystallization is not important (Bowen, 1928, pp. 299-302).

Also, during a fusion process, if the content of water is about 1 wt% or less at the time of separation of the magma from its source region, the composition of this magma will be very close to that obtained from an anhydrous source. For example, in the system Mg₂SiO₄-CaMgSi₂O₆-SiO₂-H₂O at 20 kbar (Kushiro, 1969a), a simplified anhydrous primary basalt liquid in equilibrium with a mantle source consisting of forsterite, diopside, and enstatite would have the composition 55.4% SiO₂, 15.6% CaO, 29.0% MgO by weight. An analogous liquid containing 1% H₂O and in equilibrium with the same three crystalline phases would have almost the same composition at 55.7% SiO₂, 15.5% CaO, 28.8% MgO, reduced to anhydrous proportions. This calculation assumes the approximations that the water saturated melt at this pressure contains 15 wt% water (Kushiro, 1972c) and the isobaric quaternary univariant line along which hydrous liquids are in equilibrium with forsterite, diopside, and enstatite is straight. A similar calculation for a liquid containing 1 wt% CO₂ would also produce only a very small change in the composition of the liquid, but in this case the SiO₂ content would be slightly lower than in the anhydrous melt (Eggler, 1974). Thus, for concentrations that appear to be reasonable for most geological situations, the effects of H₂O and CO₂, in addition to being very small, tend to cancel each other.

Of course, if the concentrations of volatiles at depth are much greater than those determined in basalts at the earth's surface, the above conclusions would not hold. In fact, the data of Delaney et al. (1977), Delaney et al. (in press), and Muenow et al. (submitted for publication) suggest that the H₂O content at depth is much *smaller*. They determined the

volatile content of glass-vapor inclusions in olivine and plagioclase phenocrysts from mid-ocean ridge and Hawaiian tholeiites, and found that in all cases the H₂O content was less than 0.004 wt%. Concentrations of CO₂ in the inclusions were slightly larger than in the glass surrounding the phenocrysts but were still quite small (0.2–0.4 wt%). These authors suggested that the concentrations of CO₂ and H₂O in these inclusions are a more accurate measure of conditions at depth than concentrations in the matrix glasses surrounding the phenocrysts. If this suggestion is correct, CO₂ and H₂O have virtually no influence on the compositions of tholeiitic basalts in the ocean basins. Inclusions in phenocrysts from basalts erupted in back-arc basins contain water (Muenow et al., 1977), but absolute amounts of volatiles have not yet been reported. Data on alkalic basalts are also not yet available. However, even if subsequent analyses show volatile concentrations in these other basalts to be greater than those in tholeiites from ocean basins, the effects of these volatiles could still be neglected if their concentrations do not exceed about one percent.

Acknowledgments. We wish to thank E.D. Jackson, E.F. Osborn, and H.S. Yoder, Jr. for critical review of the manuscript. This research was supported by the Earth Sciences Section, National Science Foundation, NSF Grants GA-21477 and EAR74-22571 A01.

References

- Andersen, O.: The system anorthite-forsterite-silica. *Am. J. Sci.* **39** (Fourth Ser.), 407–454 (1915)
- Anonymous: The international practical temperature scale of 1968. *Metrologia* **5**, 35–44 (1968)
- Bowen, N.L.: The ternary system diopside-forsterite-silica. *Am. J. Sci.* **38**, (Fourth Ser.), 207–264 (1914)
- Bowen, N.L.: The evolution of the igneous rocks. Princeton: Princeton Univ. Press 1928
- Boyd, F.R., England, J.L.: Apparatus for phase equilibrium measurements at pressures up to 50 kilobars and temperatures up to 1750° C. *J. Geophys. Res.* **65**, 741–748 (1960)
- Boyd, F.R., England, J.L.: Effect of pressure on the melting of diopside, CaMgSi₂O₆, and albite, NaAlSi₃O₈, in the range up to 50 kilobars. *J. Geophys. Res.* **68**, 311–323 (1963)
- Boyd, F.R., England, J.L., Davis, B.T.C.: Effects of pressure on the melting and polymorphism of enstatite, MgSiO₃. *J. Geophys. Res.* **69**, 2101–2109 (1964)
- Carmichael, I.S.E., Turner, F.J., Verhoogen, F.J.: *Igneous petrology*. New York: McGraw-Hill 1974
- Chen, C.-H., Presnall, D.C.: The system Mg₂SiO₄-SiO₂ at pressures up to 25 kilobars. *Am. Mineral.* **60**, 398–406 (1975)
- Chinner, G.A., Schairer, J.F.: The join Ca₃Al₂Si₃O₁₂-Mg₃Al₂-Si₃O₁₂ and its bearing on the system CaO-MgO-Al₂O₃-SiO₂ at atmospheric pressure. *Am. J. Sci.* **260**, 611–634 (1962)
- Clark, S.P., Jr., Schairer, J.F., de Neufville, J.: Phase relations in the system CaMgSi₂O₆-CaAl₂SiO₆-SiO₂ at low and high pressure. *Carnegie Inst. Wash. Year Book* **61**, 59–68 (1962)
- Davis, B.T.C., England, J.L.: The melting of forsterite up to 50 kilobars. *J. Geophys. Res.* **69**, 1113–1116 (1964)
- Delaney, J.R., Muenow, D., Ganguly, J., Royce, D.: Anhydrous glass-vapor inclusions from phenocrysts in oceanic tholeiite pillow basalts. *Trans. Am. Geophys. Union* **58**, 530 (1977)
- Delaney, J.R., Muenow, D.W., Graham, D.G.: Abundance and distribution of water, carbon and sulfur in the glassy rims of submarine pillow basalts. *Geochim. Cosmochim. Acta* (accepted for publication)
- Eggler, D.H.: Role of CO₂ in melting processes in the mantle. *Carnegie Inst. Wash. Year Book* **72**, 457–467 (1973)
- Eggler, D.H.: Volatiles in ultrabasic and derivative rock systems. *Carnegie Inst. Wash. Year Book* **73**, 215–224 (1974)
- Engel, A.E.J., Engel, C.G., Havens, R.G.: Chemical characteristics of oceanic basalts and the upper mantle. *Bull. Geol. Soc. Am.* **76**, 719–734 (1965)
- Gast, P.W.: Trace element fractionation and the origin of tholeiitic and alkaline magma types. *Geochim. Cosmochim. Acta* **32**, 1057–1086 (1968)
- Green, D.H.: The origin of basaltic and nephelinitic magmas in the earth's mantle. *Tectonophysics* **7**, 409–422 (1969)
- Green, D.H., Ringwood, A.E.: The genesis of basaltic magmas. *Contrib. Mineral. Petrol.* **15**, 103–190 (1967)
- Hariya, Y., Kennedy, G.C.: Equilibrium study of anorthite under high pressure and temperature. *Am. J. Sci.* **266**, 193–203 (1968)
- Hart, S.R., Nalwalk, A.J.: K, Rb, Cs and Sr relationships in submarine basalts from the Puerto Rico trench. *Geochim. Cosmochim. Acta* **34**, 145–155 (1970)
- Hytönen, K., Schairer, J.F.: The system enstatite-anorthite-diopside. *Carnegie Inst. Wash. Year Book* **59**, 71–72 (1960)
- Hytönen, K., Schairer, J.F.: The plane enstatite-anorthite-diopside and its relation to basalts. *Carnegie Inst. Wash. Year Book* **60**, 125–141 (1961)
- Ibarrola, E.: Variation trends in basaltic rocks of the Canary Islands. *Bull. Volcanol.* **33**, 729–777 (1969)
- Killingley, J.S., Muenow, D.W.: Volatiles from Hawaiian submarine basalts determined by dynamic high temperature mass spectrometry. *Geochim. Cosmochim. Acta* **39**, 1467–1473 (1975)
- Kuno, H., Yamasaki, K., Iida, C., Nagashima, K.: Differentiation of Hawaiian magmas. *Japan. J. Geol. Geog.* **28**, 179–218 (1957)
- Kushiro, I.: Compositions of magmas formed by partial zone melting of the earth's upper mantle. *J. Geophys. Res.* **73**, 619–634 (1968)
- Kushiro, I.: The system forsterite-diopside-silica with and without water at high pressures. *Am. J. Sci.* **267A**, 269–294 (1969a)
- Kushiro, I.: Discussion of the paper “the origin of basaltic and nephelinitic magmas in the earth's mantle” (D.H. Green, ed.) *Tectonophysics* **7**, 427–436 (1969b)
- Kushiro, I.: Determination of liquidus relations in synthetic silicate systems with electron probe analysis: the system forsterite-diopside-silica at 1 atmosphere. *Am. Mineral.* **57**, 1260–1271 (1972a)
- Kushiro, I.: Partial melting of synthetic and natural peridotites at high pressures. *Carnegie Inst. Wash. Year Book* **71**, 357–362 (1972b)
- Kushiro, I.: Effect of water on the composition of magmas formed at high pressures. *J. Petrol.* **13**, 311–334 (1972c)
- Kushiro, I.: Origin of some magmas in oceanic and circum-oceanic regions. *Tectonophysics* **17**, 211–222 (1973a)
- Kushiro, I.: Partial melting of garnet lherzolites from kimberlite at high pressures. In: *Lesotho Kimberlites* (P.H. Nixon, ed.), pp. 294–299. Cape Town, South Africa: Lesotho National Development Corp. 1973b
- Kushiro, I.: On the nature of silicate melt and its significance in magma genesis: regularities in the shift of the liquidus boundaries involving olivine, pyroxene, and silica minerals. *Am. J. Sci.* **275**, 411–431 (1975)
- Kushiro, I., Schairer, J.F.: New data on the system diopside-forsterite-silica. *Carnegie Inst. Wash. Year Book* **62**, 95–103 (1963)

- Kushiro, I., Yoder, H.S., Jr.: Anorthite-forsterite and anorthite-enstatite reactions and their bearing on the basalt-eclogite transformation. *J. Petrol.* **7**, 337–362 (1966)
- Kushiro, I., Yoder, H.S., Jr.: Formation of eclogite from garnet lherzolite: liquidus relations in a portion of the system $MgSiO_3$ - $CaSiO_3$ - Al_2O_3 at high pressures. *Carnegie Inst. Wash. Year Book* **73**, 266–269 (1974)
- Kushiro, I., Yoder, H.S., Jr., Mysen, B.O.: Viscosities of basalt and andesite melts at high pressures. *J. Geophys. Res.* **81**, 6351–6356 (1976)
- Lindsley, D.H.: Melting relations of plagioclase at high pressures. In: *Origin of anorthosite and related rocks* (Y.W. Isachsen, ed.), Mem. **18**, pp. 39–46. Albany, N.Y.: New York State Museum and Science Service 1968
- Macdonald, G.A.: Hawaiian petrographic province. *Bull. Geol. Soc. Am.* **60**, 1541–1595 (1949)
- Macdonald, G.A., Katsura, T.: Chemical composition of Hawaiian lavas. *J. Petrol.* **5**, 82–133
- Macdonald, G.A., Powers, H.A.: Contribution to the petrography of Haleakala volcano, Hawaii. *Bull. Geol. Soc. Am.* **57**, 115–124 (1946)
- Moore, J.G.: Water content of basalt erupted on the ocean floor. *Contrib. Mineral. Petrol.* **28**, 272–279 (1970)
- Muenow, D.W., Delaney, J.R., Meijer, A., Liu, N.: Water-rich glass-vapor inclusions in phenocrysts from tholeiitic pillow basalt rims in the Marianas back arc basin. *Trans. Am. Geophys. Union* **58**, 530 (1977)
- Muenow, D.W., Graham, D.G., Liu, N.W.K., Delaney, J.R.: Water-poor glass-vapor inclusions in phenocrysts from Hawaiian tholeiitic pillow basalts. *Earth Planet. Sci. Lett.* (submitted for publication)
- Mysen, B.O., Boettcher, A.L.: Melting of a hydrous mantle: II. Geochemistry of crystals and liquids formed by anatexis of mantle peridotite at high pressures and high temperatures as a function of controlled activities of water, hydrogen, and carbon dioxide. *J. Petrol.* **16**, 549–593 (1975)
- Mysen, B.O., Kushiro, I.: Compositional variations of coexisting phases with degree of melting of peridotite in the upper mantle. *Am. Mineral.* **62**, 843–865 (1977)
- O'Hara, M.J.: Primary magmas and the origin of basalts. *Scot. J. Geol.* **1**, 19–40 (1965)
- O'Hara, M.J.: The bearing of phase equilibria studies in synthetic and natural systems on the origin and evolution of basic and ultrabasic rocks. *Earth-Sci. Rev.* **4**, 69–133 (1968)
- O'Hara, M.J., Schairer, J.F.: The join diopside-pyroxene at atmospheric pressure. *Carnegie Inst. Wash. Year Book* **62**, 107–115 (1963)
- Osborn, E.F., Tait, D.B.: The system diopside-forsterite-anorthite. *Am. J. Sci.*, Bowen Vol., 413–433 (1952)
- Powers, H.A.: Differentiation of Hawaiian lavas. *Am. J. Sci.* **30**, (Fifth Ser.), 57–71 (1935)
- Powers, H.A.: Composition and origin of basaltic magma of the Hawaiian Islands. *Geochim. Cosmochim. Acta* **7**, 77–107 (1955)
- Presnall, D.C.: Alumina content of enstatite as a geobarometer for plagioclase and spinel lherzolites. *Am. Mineral.* **61**, 582–588 (1976)
- Presnall, D.C., Brenner, N.L., O'Donnell, T.H.: Drift of Pt/Pt10Rh and W3Re/W25Re thermocouples in single stage piston-cylinder apparatus. *Am. Mineral.* **58**, 771–777 (1973)
- Presnall, D.C., Dixon, J.R., O'Donnell, T.H., Dixon, S.A.: Origin of mid-ocean ridge tholeiites. *J. Petrology* (accepted for publication)
- Presnall, D.C., Simmons, C.L., Porath, H.: Changes in electrical conductivity of a synthetic basalt during melting. *J. Geophys. Res.* **77**, 5665–5672 (1972)
- Rucklidge, J., Gasparri, E.L.: Electron micro-probe analytical data reduction EMPADR VII. Dept. Geol. University of Toronto, unpublished (1969)
- Thompson, R.N., Esson, J., Dunham, A.C.: Major elemental chemical variations in Eocene lavas of the Isle of Skye, Scotland. *J. Petrol.* **13**, 219–253 (1972)
- Tilley, C.E.: Some aspects of magmatic evolution. *Quart. J. Geol. Soc., London* **106**, 37–61 (1950)
- Tilley, C.E., Yoder, H.S., Jr.: Pyroxene fractionation in mafic magma at high pressures and its bearing on basalt genesis. *Carnegie Inst. Wash. Year Book* **63**, 114–121 (1964)
- Williams, D.W., Kennedy, G.C.: Melting curve of diopside to 50 kilobars. *J. Geophys. Res.* **74**, 4359–4366 (1969)
- Yang, H.-Y.: Crystallization of iron-free pigeonite in the system anorthite-diopside-enstatite-silica at atmospheric pressure. *Am. J. Sci.* **273**, 488–497 (1973)
- Yoder, H.S., Jr.: Genesis of principal basalt magmas. *Carnegie Inst. Wash. Year Book* **63**, 97–101 (1964)
- Yoder, H.S., Jr.: Generation of basaltic magma. Washington, D.C.: Natl. Acad. Sci. 1976
- Yoder, H.S., Jr., Tilley, C.E.: Origin of basalt magmas: an experimental study of natural and synthetic rock systems. *J. Petrol.* **3**, 342–532 (1962)

Received June 19, 1977 / Accepted February 14, 1978